Effect of high magnetic fields on the electronic structure of density-wave systems

C. A. Balseiro* and L. M. Falicov
Department of Physics, University of California, Berkeley, California 94720
(Received 30 December 1985)

The effect of high magnetic fields on the electronic structure of some quasi-one-dimensional systems with charge- or spin-density waves is examined. Because of the specific anisotropy of the system, small electron and hole pockets created by the density wave can be destroyed by the presence of a magnetic field. This phenomenon is analyzed for various orientations of the field. The energy spectrum and the density of states in the presence of an external field are calculated for a simple quasi-one-dimensional model band structure. The effect of the magnetic field on the density-wave critical temperature is also calculated. Recent experimental results on $NbSe_3$ are analyzed in terms of this theory.

I. INTRODUCTION

The problem of the behavior of charge- and spin-density waves (CDW's and SDW's) in high magnetic fields is currently under close scrutiny.[1-7] Although these two kinds of broken-symmetry states are very different—CDW's are caused predominantly by the electron-phonon interaction and produce a charge redistribution throughout the crystal, whereas SDW's are induced by the repulsive electron-electron interaction and produce a spatially varying spin polarization—the effect of a high magnetic field on the electronic structure of CDW's and SDW's is, to a great extent, similar.

The effect of magnetic fields on the SDW systems $(TMTSF)_2X$, where X stands for PF_6 or ClO_4 and TMTSF stands for tetramethyltetraselenafulvalene has been studied experimentally[1,8,9] and theoretically.[2,3] These compounds are regarded as examples of quasi-one-dimensional (Q1D) systems. At low temperatures, they exhibit a stable SDW state. Under applied pressure, however, the SDW is destroyed: a consequence of changes in the electronic structure and in the Fermi surface. It has been reported that the application of a magnetic field perpendicular to the axis of high conductivity restores the SDW in the high-pressure regime.

Gor'kov and Lebed[2] gave the first interpretation of this remarkable effect. They showed that for a simple anisotropic metal with two open Fermi-surface sheets (corrugated planes), the tendency to SDW formation is enhanced by a magnetic field applied in a direction parallel to the sheets.

Héritier *et al.*[3,10] generalized the theory by including a magnetic-field dependence of the SDW **q** vector. They found a cascade of first-order transitions that could be observed as the magnetic field is increased.[9]

These theoretical contributions focused only on the instabilities of the normal phase, i.e., they studied the divergences of the generalized susceptibilities in the normal phase. The susceptibility $\chi_0(\mathbf{q},\mathbf{H},T)$ for various values of the **q** vector, the magnetic field **H**, and the temperature T was evaluated for some simple band structures.[10] Friedel[6] discussed these models in semiclassical terms, which is only valid for weak magnetic fields. He argued that the same effects should be observed in nearly stable CDW's as well.

Recently, an anomalous magnetic field dependence of the transport properties in the low-temperature CDW phase of $NbSe_3$ was reported.[4] It is also known that $NbSe_3$, a Q1D system, exhibits two phase transitions[11-13] associated with CDW's at $T_1=144$ K and $T_2=59$ K. In the low-temperature phase, a magnetic field perpendicular to the high-mobility b axis produces an anomalous magnetoresistance. The anomaly has been interpreted as a substantial decrease in the number of carriers caused by the magnetic field, i.e., a magnetic-field-induced obliteration of parts of the Fermi surface.[4,5] It has been shown that because of the anisotropy of the system, small electron and hole pockets created by the CDW can be destroyed by the effects of the magnetic field, resulting in an effectively better nesting of the Fermi surface.

In this contribution, we analyze the effect of high magnetic fields on the electronic structure of some Q1D systems with stable CDW's or SDW's. We also discuss the effect of the magnetic field on the critical temperatures. The model under consideration is presented in Sec. II. Section III includes the calculation and results for the electronic structure and the critical temperature. A summary and discussion are given in Sec. IV.

II. THE MODEL

The model used here to represent the Q1D system consists of a tetragonal lattice with constants $a_1 \ll a_2=a_3$, in which an electronic single s-like tight-binding band exists. The dispersion relation is given by

$$E_0(\mathbf{k})=-2t\cos(k_x a_1)-2t'[\cos(k_y a)+\cos(k_z a)] -4t''\cos(k_y a)\cos(k_z a)\ , \tag{2.1}$$

where $\mathbf{k}=(k_x,k_y,k_z)$ and $a=a_2=a_3$. The parameters t and t' are the electron-transfer matrix elements between nearest neighbors in the x direction and in the (y,z) plane, respectively; t'' is the electron-transfer matrix element be-

tween second-nearest neighbors in the (y,z) plane. Because of the Q1D character of the system, $t \gg t',t''$.

Except for energies close to either the bottom or the top of the band, the surfaces of constant energy in $\mathbf{k}$ space are given by two open, corrugated sheets. The system shows a tendency to form density waves (DW's) with a wave vector $\mathbf{q}$ which connects (nests) the two open sheets of Fermi surface. The stable DW is either a CDW or an SDW, depending on the number of electrons and on the strength of the electron-phonon and the repulsive electron-electron interactions.[14]

If the electron density is taken to be one electron per site, the two pieces of Fermi surface are centered at $k_x \cong \pm(\pi/2a_1)$. For $t'' \ll t'$, the DW instability occurs for $\mathbf{q}=(\pi/a_1,\pi/a,\pi/a)$. The DW is characterized by a gap order parameter τ. Because of the extra periodicity induced in the system by the DW, the one-electron state $|\mathbf{k}\rangle$ is mixed with the state $|\mathbf{k}+\mathbf{q}\rangle$; the matrix element of this mixing is proportional to τ, a quantity assumed to be independent of $\mathbf{k}$.

The total Hamiltonian in second quantization takes the form

$$H=H_0+H_1(\tau) , \tag{2.2}$$

where

$$H_0=\sum_{\mathbf{k},\sigma} E_0(\mathbf{k})c^{\dagger}_{\mathbf{k}\sigma}c_{\mathbf{k}\sigma} , \tag{2.3}$$

$$H_1=\sum_{\mathbf{k},\sigma} \tau_\sigma c^{\dagger}_{\mathbf{k}\sigma}c_{(\mathbf{k}+\mathbf{q})\sigma} . \tag{2.4}$$

The operator $c^{\dagger}_{\mathbf{k}\sigma}$ creates an electron with crystal momentum $\mathbf{k}$ and spin σ, and

$$\tau_\uparrow=\tau_\downarrow=\tau \text{ for CDW's} ,$$

$$\tau_\uparrow=-\tau_\downarrow=\tau \text{ for SDW's} .$$

The DW quasiparticle spectrum of the system is given by

$$E_\pm(\mathbf{k})=-4t''\cos(k_y a)\cos(k_z a) \pm(\{2t\cos(k_x a_1) +2t'[\cos(k_y a)+\cos(k_z a)]\}^2+\tau^2)^{1/2} . \tag{2.5}$$

For $t''=0$, this energy spectrum has a gap 2τ at the center of the band, i.e., at the Fermi level. The DW phase is therefore a semiconductor. This fact is a consequence of the perfect nesting of the normal, $\tau=0$ Fermi surface.

For $t''\neq 0$, there is no longer perfect nesting. As before, the DW induces a *direct gap* of value 2τ. But the spectrum now has a smaller *indirect gap* of value $2\Delta_g$ given by

$$\Delta_g=\begin{cases}\tau-4t'' & \text{if } \tau/t''>4 ,\\ 0 & \text{otherwise.}\end{cases} \tag{2.6}$$

In this case, depending on the value of τ/t'', the sytem in the presence of a DW is either a semiconductor or a semimetal.

When a magnetic field is applied, new complications arise. Whereas the DW causes gaps in an otherwise continuous spectrum, the magnetic field quantizes the electronic motion in the two directions perpendicular to it and tends to form either discrete levels and narrow bands if the cyclotron electronic orbits are closed, or complicated continua if they are open.[15–19] The competition between these various effects are the cause of the strange, complex behavior under study here.

For low magnetic fields, a simple semiclassical description of the motion of the electrons can be used. This scheme, according to Onsager's quantization rules,[15] yields only allowed closed electron and hole orbits which enclose an integral number of magnetic field flux quanta. Open orbits, which arise from the combined effect of magnetic field and periodic potential, form a continuum and are not quantized in the traditional sense. This approach completely neglects several secondary effects: band broadening, tunneling between bands, and the complicated structure of the continuum. These effects are of considerable importance in the case under study. Were it not for the presence of the gap parameter τ, the spectrum of the model would yield only open orbits, i.e., a continuum in Onsager's scheme; the gap parameter τ, on the other hand, may be of the same order of the magnitude of the cyclotron energy $\hbar\omega_c$ of the closed electron or hole orbits (induced by τ) for reasonbly attainable values of the magnetic field.

An acceptable scheme to describe the DW and the effects of the magnetic field on equal footing can be obtained from the well-known effective-mass theory of Luttinger and Kohn.[20] If paramagnetic (spin) effects are neglected, the Hamiltonian of the system in first quantization is given by

$$H=H_0(\boldsymbol{\kappa})+H_1(\tau) , \tag{2.7}$$

where the first term is obtained from (2.1),

$$H_0(\boldsymbol{\kappa})=E_0(\mathbf{k}=\boldsymbol{\kappa}) , \tag{2.8}$$

with the differential operator $\boldsymbol{\kappa}$ defined by

$$\boldsymbol{\kappa}=-i\nabla+(|e|/\hbar c)\mathbf{A}(\mathbf{r}) , \tag{2.9}$$

and the second term describes the perturbations induced by the DW. For a uniform magnetic field $\mathbf{H}=(0,H_y,H_z)$ perpendicular to the x direction, the vector potential takes the form

$$\mathbf{A}(\mathbf{r})=(0,-H_z x,H_y x) . \tag{2.10}$$

In this gauge, the total Hamiltonian in second quantization can be written

$$H=\sum_{n,k_\rho,\sigma}\varepsilon(n,k_\rho)c^{\dagger}_{nk_\rho\sigma}c_{nk_\rho\sigma}-t\sum_{n,k_\rho,\sigma}\sum_{\delta=\pm1}c^{\dagger}_{nk_\rho\sigma}c_{(n+\delta)k_\rho\sigma} +\sum_{n,k_\rho,\sigma}\tau_\sigma\cos(nq_x a_1)c^{\dagger}_{nk_\rho\sigma}c_{n(k_\rho+q_\rho)\sigma} . \tag{2.11}$$

Here, k_ρ (q_ρ) is a two-dimensional vector with components k_y and k_z (q_y,q_z). The index n refers to the atomic planes perpendicular to the x direction and the operator $c^{\dagger}_{nk_\rho\sigma}$ creates an electron in the state $|nk_\rho\sigma\rangle$ of energy $\varepsilon(n,k_\rho)$ given by

$$\varepsilon(n,k_\rho)=-2t'[\cos(k_y a+\Phi_z n)+\cos(k_z a+\Phi_y n)] -4t''\cos(k_y a+\Phi_z n)\cos(k_z a+\Phi_y n)\ , \quad (2.12)$$

where

$$\Phi_I=(|e|/\hbar c)H_I a_1 a \quad (I=y,z)\ . \quad (2.13)$$

The effective Hamiltonian for the magnetic field along the x direction is obtained in a similar way. Since the vector potential is now (depending on the gauge) a function of either y or z, the substitution of $\mathbf{k}$ in (2.1) by the operator $\boldsymbol{\kappa}$ given by (2.9) yields two cosine operators that do not commute, and therefore an "ambiguous" Hamiltonian. If the Hermitian (symmetrized) product of the two cosines is taken, the resulting Hamiltonian is

$$H=\sum_{n,k_\rho,\sigma}\varepsilon(n,k_\rho)c^\dagger_{nk_\rho\sigma}c_{nk_\rho\sigma} -\sum_{n,k_\rho,\sigma}[t^+(n,k_\rho)c^\dagger_{nk_\rho\sigma}c_{(n+1)k_\rho\sigma} +t^-(n,k_\rho)c^\dagger_{nk_\rho\sigma}c_{(n-1)k_\rho\sigma}] +\sum_{n,k_\rho,\sigma}\tau_\sigma\cos(nq_z a)c^\dagger_{nk_\rho\sigma}c_{n(k_\rho+q_\rho)\sigma}\ , \quad (2.14)$$

where $k_\rho=(k_x,k_z)$,

$$\varepsilon(n,k_\rho)=-2t\cos(k_x a_1)-2t'\cos(k_z a+\Phi n)\ , \quad (2.15)$$

$$t^\pm(n,k_\rho)=t'+t''\{\cos[k_z a+\Phi(n\pm1)] +\cos(k_z a+\Phi n)\}\ , \quad (2.16)$$

$$\Phi=(|e|H/\hbar c)a^2\ . \quad (2.17)$$

Results for the energy spectrum for magnetic fields along [001], [011], and [100] are shown in the next section.

III. CALCULATIONS AND RESULTS

A. Semiclassical results

For low magnetic fields, a simple semiclassical description of the motion of the quasiparticles and Onsager's quantization scheme[15] are adequate. Although this procedure neglects several important effects, it is instructive as a first approximation to this complex problem.

The motion of the quasiparticles along the direction of the magnetic field is not affected by the presence of the field, and consequently the crystal momentum along the direction of $\mathbf{H}$ is a good quantum number. In $\mathbf{k}$ space, the orbits are defined by the lines of constant energy in the two-dimensional (2D) band structure corresponding to any plane perpendicular to the magnetic field direction. In the direction perpendicular to the field, the allowed semiclassical trajectories are determined by Onsager's scheme, which requires that the closed semiclassical trajectories enclose $(n+\frac{1}{2})$ magnetic flux quanta, where $n=0,1,2,\ldots$. Open orbits are not quantized. This scheme yields a continuum in the region of open orbits, and highly degenerate, discrete states (the Landau levels) in regions of closed orbits.

For the simple tetragonal band structure in the presence of a DW and for a magnetic field along [001], the 2D band structure contains, near the Fermi level, four Van-Hove singularities, two in the valance band (a saddle point T_{v1} and a maximum T_{v2}) and two in the conduction band (a minimum T_{c0} and a saddle point T_{c1}). These singularities correspond in the density of states to finite discontinuities (for T_{v2} and T_{c0}) or to logarithmic divergences (for T_{v1} and T_{c1}). For a given value of k_z, the energies associated with these singularities are,

$$E(T_{c0})=-E(T_{v2})=\begin{cases}-4t''\cos(k_z a)+\tau & \text{if } |k_z|\leqq(\pi/2a)\ ,\\ 4t''\cos(k_z a)+\tau & \text{if } |k_z|\geqq(\pi/2a)\ ,\end{cases} \quad (3.1)$$

$$E(T_{c1})=-E(T_{v1})=\begin{cases}4t''\cos(k_z a)+\tau & \text{if } |k_z|\leqq(\pi/2a)\ ,\\ -4t''\cos(k_z a)+\tau & \text{if } |k_z|\geqq(\pi/2a)\ .\end{cases} \quad (3.2)$$

Depending on the values of the parameters and on the k_z section under consideration, there are two possible orderings for these energies, either

$$E(T_{v1})<E(T_{c0})<E(T_{v2})<E(T_{c1}) \quad (3.3)$$

or

$$E(T_{v1})<E(T_{v2})<E(T_{c0})<E(T_{c1})\ . \quad (3.4)$$

In either case, there are only open orbits in the valence band for $E<E(T_{v1})$ and only open orbits in the conduction band for $E>E(T_{c1})$. If the ordering is that of (3.3), i.e., a semimetallic 2D section, there are closed hole orbits only for $E(T_{v1})<E<E(T_{c0})$; both closed electron and closed hole orbits for $E(T_{c0})<E<E(T_{v2})$; closed electron orbits only for $E(T_{v2})<E<E(T_{c1})$. If the ordering is that of (3.4), i.e., a semiconducting 2D section, there are closed hole orbits only for $E(T_{v1})<E<E(T_{v2})$; no states at all (a gap) for $E(T_{v2})<E<E(T_{c0})$; closed electron orbits only for $E(T_{c0})<E<E(T_{c1})$.

In the presence of a magnetic field, there are continua for $E<E(T_{v1})$ and for $E>E(T_{c1})$. For $E(T_{v1})<E<E(T_{c1})$ there are either only discrete Landau levels or no states at all, depending on the values of the band parameters and the value of the magnetic field.

It has been shown[18] that broadening effects caused by the lattice periodic potential are important for those Landau levels with energies close to that of a saddle point. Onsager's scheme neglects this broadening. For our model, this effect would call for considerable broadening only for those energies slightly larger than $E(T_{v1})$ and those slightly smaller than $E(T_{c1})$.

This analysis can be carried out for any 2D section and

for any orientation of the magnetic field, and depends only on the values of the energies at the 2D Van Hove singularities.

B. Energy spectrum: exact results

From the Hamiltonian obtained in Sec. II, it is clear that the magnetic field induces a new periodicity in the system. The problem of Bloch electrons in a magnetic field has been studied intensively and extensively.[15–19] The physical properties of the system do not depend, except on an extremely fine scale, on the commensurability of the magnetic-field-induced and the lattice periodicities. Within this framework it is possible then, without loss of generality, to restrict oneself to the case of "rational" fields, in particular, to values of Φ_I or Φ of (2.13) and (2.16) equal to $2\pi/N$, where N is a large integer.

As shown in Appendix A, the energy spectrum for each value of k_ρ can be obtained by evaluating the eigenvalues of the transfer matrix. The total energy spectrum is a superposition of the spectra obtained for all values of k_ρ in the two-dimensional Brillouin zone.

For a magnetic field along the z direction the 2D energy spectra for $E>0$ and various values of k_z are shown in Fig. 1. The spectra for $E<0$ are very nearly the same. The numerically exact method employed in the calculation is slowly convergent and no longer practical for small values of the magnetic field ($N>2000$). For small magnetic fields, more efficient approximation methods should be used. Interpolation between the lowest calculated values and $H=0$ is easily accomplished, and is shown as an example in Fig. 1(a). Results can be summarized as follows.

(i) For low magnetic fields, the semiclassical spectra are reproduced.

(ii) For intermediate and high fields, there is a substantial broadening of all Landau levels.

(iii) For high magnetic fields, electron and hole levels are very broad, and the lowest (highest) boundary of the broadened $n=0$ electron (hole) level is at an energy very close to τ ($-\tau$). As a consequence, the total three-dimensional spectra for high magnetic fields have a gap for energies $|E|<\tau$ and a continuum of states for $|E|>\tau$. All k_z sections contribute no states for $|E|<\tau$ and continuum states for $|E|>\tau$, just as in the perfect nesting case.

(iv) For energies $E>E(T_{c1})$ and $E<E(T_{v1})$, the spectra still exhibit broad levels (bands) separated by small gaps. A gapless continuum is only recovered for $E\gg E(T_{c1})$ and for $E\ll E(T_{v1})$.

The very large broadening of the Landau levels, in particular the $n=0$ levels, and the existence of gaps in the semiclassical continuum can be understood only in terms of a magnetic-field-induced mixing of electronic bands, i.e., a hybridization of the valence and conduction bands. This mixing is important if the magnetic cyclotron energy $\hbar\omega_c$ is of the same order of magnitude of the gap parameter τ. In fact, the proper scale to measure the magnetic field strength is not Φ (which measures the ultrafine structure), by the cyclotron energy

$$\hbar\omega_c=\hbar|e|H/m^*c\ , \tag{3.5}$$

with an effective mass m^* corresponding to the bottom of the DW-state conduction band

$$m^*=(\hbar^2/4a_1a_2)\{\tau/t''[t^2-4(t')^2]\}^{1/2}\ . \tag{3.6}$$

It can be seen that if the condition $t\gg t'\gg t''$ is maintained, the energy spectrum is only sensitive to the ratios $\hbar\omega_c/t''$ and τ/t''.

For a high magnetic field, the spectrum has a large gap at the center of the band, i.e., the Fermi level. This central gap $2\Delta_g$ is of the order of 2τ, even for values of $\tau/t''\leqq 4$. As the magnetic field is reduced, the size of the central gap decreases and vanishes for a given value of the field which depends on τ. For magnetic fields smaller than this value, there is a band of allowed continuum states at the center of the spectrum and the system is semimetallic.

Figure 2 is a diagram of constant energy-gap parameter

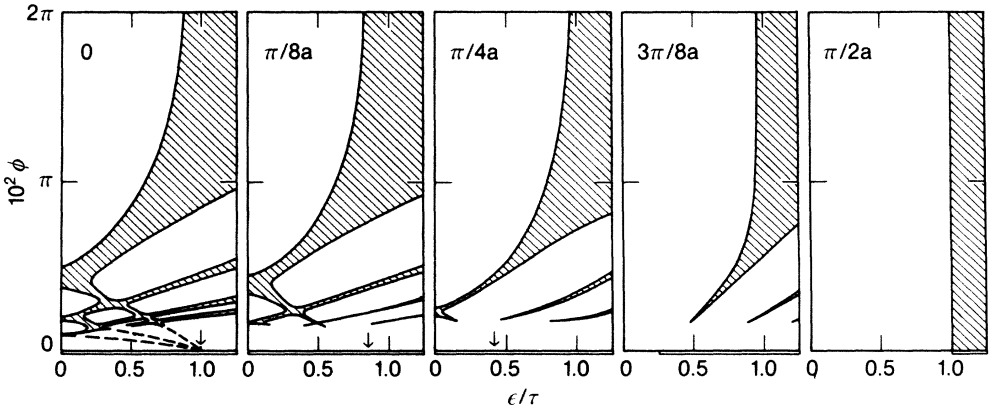

FIG. 1. Energy spectra for magnetic fields parallel to [001], $E>0$ (the conduction band) and various values of k_z. The abscissae are energies and the ordinates the magnetic field strength. Near the abscissa axis, the numerical method described in the text converges very slowly. Extrapolation to $H\to 0$ of the first few hole levels (dashed lines) is shown in for $k_z=0$. The semiclassical Van Hove singularities are indicated along the energy axis and by arrows. The broadened Landau levels can be recognized in all sections.

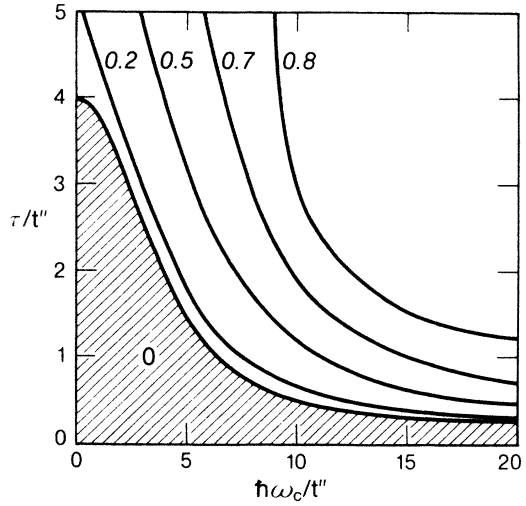

FIG. 2. The values of Δ_g/τ as a function of magnetic field $\hbar\omega_c/t''$ and τ/t'' for **H** parallel to [001], $t'/t=0.2$, and $t''\ll t'$. The shaded region corresponds to $\Delta_g=0$ and band overlap, the semimetallic case. The gap increases rapidly to its maximum value $\Delta_g=\tau$. Note that for all parameter values, a semiconducting state is obtained if the field strength is large enough.

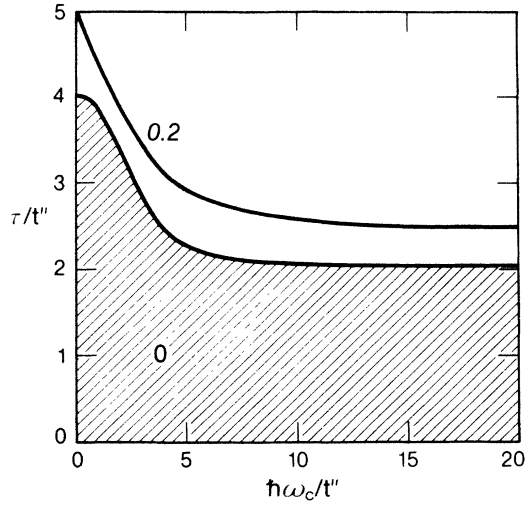

FIG. 3. The values of Δ_g/τ as a function of magnetic field $\hbar\omega_c/t''$ and τ/t'' for **H** parallel to [011], $t'/t=0.2$, and $t''\ll t'$. The shaded region corresponds to $\Delta_g=0$ and band overlap, the semimetallic case. The gap increases rapidly to its maximum value $\Delta_g=\tau$. Note that only for $\tau/t''>2$, a semiconducting state is obtained if the field strength is large enough. For $\tau/t''<2$ the system is always semimetallic, regardless of magnetic field strength.

Δ_g/τ in the $(\hbar\omega_c/t'',\tau/t'')$ plane. For $\tau/t''<4$, there is a two-dimensional region of the plane corresponding to a semimetallic regime, $\Delta_g=0$. The high-magnetic-field region is semiconducting, with the energy-gap parameter increasing monotonically with either variable.

Because of the intricate fine structure of the spectrum, characteristic of Bloch electrons in a magnetic field, a very small gap could appear at the Fermi level in the semimetallic regime for some particular values of the magnetic field. These are in general very small gaps of a different nature that are completely obliterated by small inhomogeneities in the field and that do not change the physical properties of the system.

A magnetic field along [011] produces similar but less pronounced effects. Figure 3 is a diagram of constant energy gap for this case. Any reasonable high magnetic field produces now a semiconducting state only for $\tau/t''>2$.

Energy spectra for magnetic fields along the high-conductivity [100] x axis are evaluated in the same fashion, with the use of the Hamiltonian (2.14)–(2.17). For the field in this direction, no central gaps are obtained if $\tau/t''<4$.

C. Density of states

A magnetic field along [001] can produce important changes in the energy spectrum of the system. It is instructive to study the behavior of the density of states as the magnetic field increases. In what follows, numerical results for the density of states in the region of interest, i.e., the center of the band, are presented.

The total density of states per spin is given by

$$D_\sigma(E)=(-1/\pi)\lim_{\eta\to 0}\sum_{n,k_\rho}\mathrm{Im}G_{nk_\rho\sigma}(E+i\eta)\ , \tag{3.7}$$

where Im indicates the imaginary part and $G_{nk_\rho\sigma}$ is a Green's function, given by

$$G_{nk_\rho\sigma}(E+i\eta)=\langle\langle c_{nk_\rho\sigma},c^{\dagger}_{nk_\rho\sigma}\rangle\rangle_{E+i\eta}\ . \tag{3.8}$$

The method used to evaluate G is described in Appendix B. Densities of states at the center of the band for three different values of the magnetic field along the [001] direction are shown in Fig. 4. Figure 4(a) corresponds to a value of the field in the semimetallic regime; a complex structure characteristic of Bloch electrons in a magnetic field is readily apparent. Higher values of the magnetic field are presented in Figs. 4(b) and 4(c), where Δ_g/τ attains the values 0.38 and 0.85, respectively. The small tails in $D_\sigma(E)$ which can be observed near the gap edges are a consequence of the finite imaginary part η of the energy used in the numerical evaluations. Except for the fine-structure details, the densities of states at high magnetic fields resemble that of the system with perfect Fermi-surface nesting, i.e., no k_z section contributes states to the $|E|<\tau$ region of the spectrum. Contrary to the predictions of the semiclassical model, there is a real gap in the spectrum.

D. Critical temperature

The order parameter τ must be calculated self-consistently, and is, in general, a function of the direction and the strength of the magnetic field. The equilibrium value of τ is given by

$$\tau=\lambda\sum_{n,k_\rho}\cos(nq_xa_1)\langle c^{\dagger}_{nk_\rho\sigma}c_{n(k_\rho+q_\rho)\sigma}\rangle\ , \tag{3.9}$$

where λ is the interaction parameter and $\langle\cdots\rangle$ indicates thermodynamic averages. A self-consistent calculation

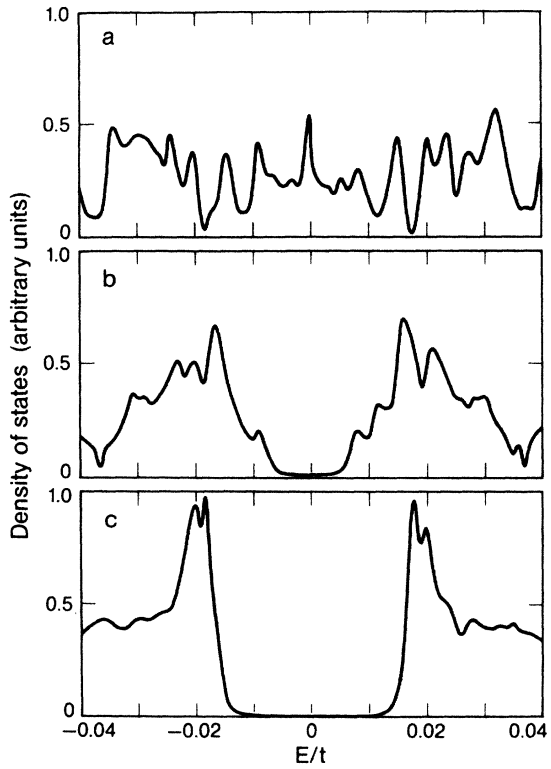

FIG. 4. Total three-dimensional densities of states near the Fermi level for magnetic fields parallel to [001] and various values of the field strength. (a) Semimetallic regime $\hbar\omega_c/\tau=2.03$ ($N=400$); (b) semiconducting regime $\hbar\omega_c/\tau=4.07$ ($N=200$) with $\Delta_g/\tau=0.38$; (c) semiconducting regime $\hbar\omega_c/\tau=8.14$ ($N=100$) with $\Delta_g/\tau=0.85$.

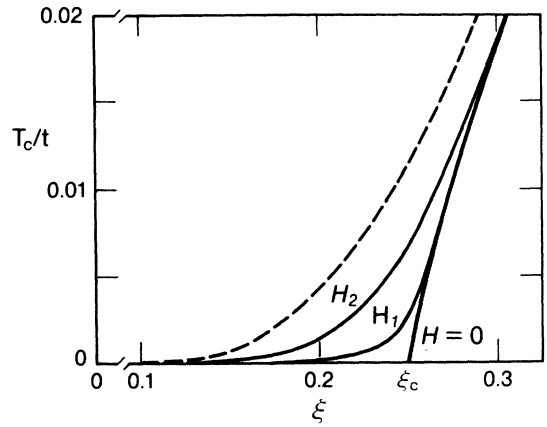

FIG. 5. The critical temperature T_c as a function of interaction strength ξ for (a) the perfect nesting case $t''=0$ and $H=0$ (dashed line); (b) a semimetallic case $t''=0.01t$ and $H=0$ (observe the critical value ξ_c); the case shown in (b) for magnetic fields parallel to [001], strength such that (c) $N=400$ and (d) $N=200$. It should be noted that T_c changes appreciably with magnetic field strength only for ξ in the vicinity of ξ_c. For the lattice parameters of $NbSe_3$, $N=400$ corresponds to $H\approx 250$ kG.

with the present model is a tedious and numerically expensive proposition which has not been carried out. Two extreme situations can, however, be readily analyzed. At $T=0$, the self-consistent solution of (3.9) can be obtained by minimizing the total energy

$$E_T=\sum_\sigma \int_{-\infty}^{\varepsilon_F} D_\sigma(E)E\,dE-\tau^2/2\lambda\ , \tag{3.10}$$

where ε_F is the Fermi level. Since the density of states $D_\sigma(E)$ for high magnetic fields along [001] resembles that characteristic of the system with perfect Fermi-surface nesting, the order parameter τ for this limiting case must be numerically close to that obtained in the perfect-nesting case.

The critical temperature and its magnetic field dependence can also be calculated in a simple way. A linearization of the dispersion relation (2.1) for k_x in the vicinity of $\pm(\pi/2a_1)$ and the procedure described in Ref. 2 yields, for the magnetic field in the [001] direction, the following equation for the critical temperature T_c:

$$1=\frac{\lambda}{4\pi t a_1 a^2}\int_{\pi T_c/t}^{\infty} dy\frac{1}{\sinh y} \times J_0^2((4t''/t\Phi)\sin(yt\Phi/2\pi T_c))\ , \tag{3.11}$$

where $\Phi=\Phi_z$ of (2.13) and J_0 is the ordinary Bessel function.

In Fig. 5, the critical temperature T_c as a function of the dimensionless coupling constant $\xi=\lambda/4\pi t a_1 a^2$ is shown. Because of the lack of perfect nesting at $H=0$, the DW is stable only for $\xi>\xi_c$, a minimum critical value of the interaction. A magnetic field, however, can induce a DW for $\xi>\xi_c$. This magnetic-field-induced DW was predicted by Gor'kov and Lebed.[2] For $\xi>\xi_c$, the presence of a magnetic field raises the value of T_c. However, if the critical temperature for zero magnetic field is not too low, T_c does not change appreciably with magnetic field. This effect is shown in Fig. 6, where T_c is plotted against magnetic field strength for fields along [001] and for various values of ξ. The critical temperature increases monotonically with the field.

For magnetic fields along [011], the 2D band structure becomes equivalent to that used in Ref. 2. The increase in T_c for this direction of the field shows oscillatory behavior. Here again, the effect of the magnetic field is important only for values of ξ close to the critical value ξ_0, i.e., for anisotropic DW systems which are either marginally stable or marginally unstable.

IV. SUMMARY AND DISCUSSION

The effect of a magnetic field on the electronic structure of some Q1D systems with a CDW or an SDW has been examined. The system is characterized by a well-defined **q** vector and by a lack of perfect nesting which result, at zero field, in a semimetallic system. The results can be summarized as follows.

(a) A magnetic field perpendicular to the axis of high conductivity may induce gaps in the spectrum at the Fermi level, thus transforming a semimetallic structure into a

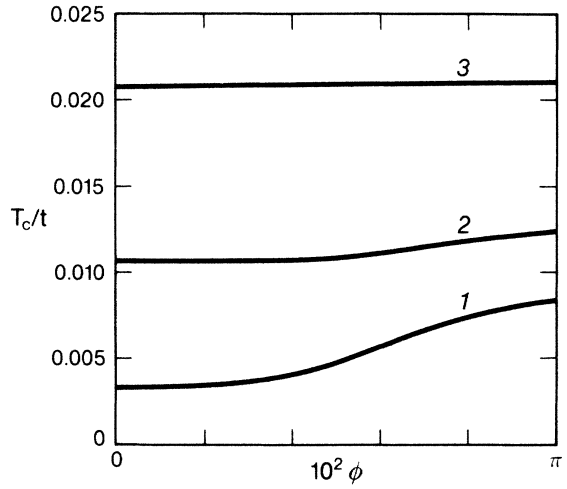

FIG. 6. The DW transition temperature T_c as a function of magnetic field strength for fields parallel to [001] and various values of the interaction parameter ξ. Notice that T_c increases monotonically with field strength, but the increase is sizable only for ξ in the vicinity of ξ_c.

semiconducting one.

(b) The value of the gap Δ_g is a function of the DW strength τ, the cyclotron energy $\hbar\omega_c$, and the "lack of nesting" parameter t'', but insensitive to other band-structure parameters.

(c) Although at low magnetic fields the spectrum of the system is well described by the semiclassical quantization scheme, this scheme breaks down for fields such that the cyclotron energy is of the order of, or greater than the DW mixing parameter τ; in the latter regime band mixing becomes paramount.

(d) The complete spectrum of the system as a function of the various parameters shows two main effects: (1) in the semiclassical (closed orbit) discrete regime the Landau levels spread into wider and wider bands as the field strength increases, and (2) in the semiclassical (open orbit) continuum energy gaps appear at high fields.

(e) The semimetal-to-semiconductor transition does not take place for magnetic fields parallel to the axis of high conductivity, the x axis in the simple model.

(f) There is also considerable anisotropy for fields perpendicular to the high-conductivity axis [the (y,z) plane]. For fields along the $\langle 001\rangle$ axes, semimetal-to-semiconductor transitions are obtained for high enough field strength regardless of the value of the ratio τ/t''. For fields along $\langle 011\rangle$ axes, the semiconducting gap does not open up at any field strength if the ratio τ/t'' is smaller than a given value (2 in this model).

(g) The DW transition temperature T_c is, in this model, enhanced by the magnetic field.[21] The enhancement, however, is only appreciable if the situation is such that the interaction strength ξ is just below or just above the critical value ξ_c, i.e., for marginally stable or marginally unstable,[2] semimetallic DW's. For well-established, stable DW's, the enhancement effect is small.

(h) All effects encountered in this tetragonal model can be directly applied to interpret the experiments in the more anisotropic, real systems such as $NbSe_3$ (a CDW system) or the TMTSF salts (SDW's). The complexity of the spectra and electronic effects found here are complicated even more by the complexity of the real band structure in these materials, where several sheets of Fermi surface (of various topologies) contribute to the conduction process.

ACKNOWLEDGMENTS

The author's are deeply indebted to Professor R. V. Coleman for many illuminating and challenging discussions, and for keeping them informed on a day-to-day basis of the results of his experiments. This work was supported by the National Science Foundation through Grant No. DMR-81-06494. One of the authors (C.A.B.) would like to acknowledge the financial support from the John Simon Guggenheim Memorial Foundation (New York, NY) and from the Centro Atómico Bariloche (Argentina).

APPENDIX A: THE TRANSFER MATRIX

The transfer-matrix method used to calculate the energy spectrum for **H** along the z axis is described here. For a given value of k_ρ, the Hamiltonian is diagonalized by defining a quasiparticle creation operator

$$a^\dagger_{\nu k_\rho\sigma}=\sum_n[\alpha(\nu,n;k_\rho\sigma)c^\dagger_{nk_\rho\sigma}+\beta(\nu,n;k_\rho\sigma)c^\dagger_{n(k_\rho+q_\rho)\sigma}]\ , \tag{A1}$$

which satisfies the equation of motion

$$[a^\dagger_{\nu k_\rho\sigma},H]=-Ea^\dagger_{\nu k_\rho\sigma}\ . \tag{A2}$$

Equation (A2) is used to determine the coefficients α and β of (A1). For that purpose, the following matrix method is employed:

$$A_{n+1}(k_\rho,\sigma)=T_n(k_\rho)A_n(k_\rho,\sigma)\ , \tag{A3}$$

where the column vector $A_n(k_\rho,\sigma)$ is defined by

$$A_n(k_\rho,\sigma)\equiv\begin{bmatrix}\alpha(\nu,n;k_\rho\sigma)\\ \alpha(\nu,n-1;k_\rho\sigma)\\ \beta(\nu,n;k_\rho\sigma)\\ \beta(\nu,n-1;k_\rho\sigma)\end{bmatrix} \tag{A4}$$

and the transfer matrix $T_n(k_\rho)$ is given by

$$T_n(k_\rho)=\begin{bmatrix}\varepsilon(n,k_\rho)-E & -t & \tau_n & 0\\ 1 & 0 & 0 & 0\\ \tau_n & 0 & \varepsilon(n,k_\rho+q_\rho)-E & -t\\ 0 & 0 & 1 & 0\end{bmatrix}, \tag{A5}$$

where

$$\tau_n=\tau_\sigma\cos(nq_xa)=(-1)^n\tau_\sigma\ . \tag{A6}$$

The coefficients associated with a given n can be obtained in terms of those associated with $n=0$ by repeated application of the T matrix

$$A_n(k_\rho,\sigma)= T_{n-1}(k_\rho)T_{n-2}(k_\rho) \times \cdots T_1(k_\rho)T_0(k_\rho)A_0(k_\rho,\sigma) . \quad \text{(A7)}$$

For values of the magnetic field such that $\Phi_z=2\pi/N$, with N an even number, the combined lattice-magnetic-field periodicity of the system in the x direction is given by Na_1. The use of Bloch's theorem yields the important result that an eigenstate of the system with energy E exists if the product of N transfer matrices has a complex eigenvalue ζ in the complex-plane unit circle, i.e., an eigenvalue of modulus one. The use of (A5) gives, for the eigenvalue equation, a quartic of the form

$$\zeta^4-A\zeta^3-B\zeta^2-A\zeta+1=0 . \quad \text{(A8)}$$

With the definitions

$$\eta_\pm=-(A^2/4)\pm\tfrac{1}{2}[(A^2/4)+2+B]^{1/2} , \quad \text{(A9)}$$

it is easy to show that the eigenstate condition is satisfied if either η_+ or η_- is a real number such that $-1<\eta_\pm<1$.

This procedure needs to be repeated for each value of k_ρ.

APPENDIX B: GREEN'S FUNCTIONS

The Green's functions of the system were calculated only for values of the magnetic field such that $\Phi_z=2\pi/N$, with N an even number. The combined periodicity of the field and lattice systems is then Na_1 along the x axis. The following Green's function matrix is defined

$$\hat{G}_{nn'}\equiv \begin{bmatrix} \langle\langle c_{nk_\rho\sigma}, c^\dagger_{n'k_\rho\sigma}\rangle\rangle_{E+i\eta} & \langle\langle c_{nk_\rho\sigma}, c^\dagger_{n'(k_\rho+q_\rho)\sigma}\rangle\rangle_{E+i\eta} \\ \langle\langle c_{n(k_\rho+q_\rho)\sigma}, c^\dagger_{n'k_\rho\sigma}\rangle\rangle_{E+i\eta} & \langle\langle c_{n(k_\rho+q_\rho)\sigma}, c^\dagger_{n'(k_\rho+q_\rho)\sigma}\rangle\rangle_{E+i\eta} \end{bmatrix} . \quad \text{(B1)}$$

The equations of motion for $\hat{G}_{nn'}$ are given by

$$\begin{aligned} \hat{G}_{00}&=\hat{g}_0+\hat{g}_0(\hat{T}\hat{G}_{10}+\hat{T}\hat{G}_{-10}) , \\ \hat{G}_{\pm10}&=\hat{g}_{\pm1}(\hat{T}\hat{G}_{00}+\hat{T}\hat{G}_{\pm20}) , \\ \hat{G}_{\pm20}&=\hat{g}_{\pm2}(\hat{T}\hat{G}_{\pm10}+\hat{T}\hat{G}_{\pm30}) , \end{aligned} \quad \text{(B2)}$$

etc., where

$$\hat{g}_n=\{[E+i\eta-\varepsilon(n,k_\rho)][E+i\eta-\varepsilon(n,k_\rho+q_\rho)]-\tau^2\}^{-1} \begin{bmatrix} E+i\eta\varepsilon(n,k_\rho+q_\rho) & \tau_n \\ \tau_n & E+i\eta-\varepsilon(n,k_\rho) \end{bmatrix} , \quad \text{(B3)}$$

and

$$\hat{T}=\begin{bmatrix} t & 0 \\ 0 & t \end{bmatrix} . \quad \text{(B4)}$$

Elimination of $\hat{G}_{\pm10}$ from the (B2) system of equations yields

$$\begin{aligned} \hat{G}_{00}&=\tilde{g}_0+\tilde{g}_0(\tilde{T}_+\hat{G}_{20}+\tilde{T}_-\hat{G}_{-20}) , \\ \hat{G}_{\pm20}&=\tilde{g}_{\pm2}(\tilde{T}_\pm\hat{G}_{00}+\hat{T}\hat{G}_{\pm30}) , \\ \hat{G}_{\pm30}&=\hat{g}_{\pm3}(\hat{T}\hat{G}_{\pm20}+\hat{T}\hat{G}_{\pm40}) , \end{aligned} \quad \text{(B5)}$$

etc., where

$$\tilde{g}_0=(1-\hat{g}_0\hat{T}\hat{g}_1\hat{T}-\hat{g}_0\hat{T}\hat{g}_{-1}\hat{T})^{-1}\hat{g}_0 , \quad \text{(B6)}$$

$$\tilde{g}_{\pm2}=(1-\hat{g}_2\hat{T}\hat{g}_{\pm1}\hat{T})^{-1}\hat{g}_{\pm2} , \quad \text{(B7)}$$

and

$$\tilde{T}_\pm=\hat{T}\hat{g}_{\pm1}\hat{T} . \quad \text{(B8)}$$

Repetition of this procedure $(N-1)$ times gives $\hat{G}_{00}$ directly connected with $\hat{G}_{\pm N0}$. In a similar way $\hat{G}_{\pm N0}$ can be directly connected with $\hat{G}_{00}$ and $\hat{G}_{\pm2N0}$, etc. Since the locations $0,\pm N,\pm2N,\ldots$ are all equivalent by translational symmetry, the remaining equations can be easily solved by Fourier transformation. It was found, however, that for numerical calculations, it is convenient to use a lattice decimation procedure[22] which converges more rapidly.

*On leave from Centro Atómico Bariloche, Comisión Nacional de Energía Atómica, 8400 San Carlos de Bariloche, Rio Negro, Argentina.

[1]R. Brusetti, P. Garoche, and K. Bechgaard, J. Phys. C **16**, 3535 (1983).

[2]L. P. Gor'kov and A. G. Lebed, J. Phys. (Paris) Lett. **45**, L433 (1984).

[3]M. Héritier, G. Mantambaux, and P. Lederer, J. Phys. (Paris) Lett. **45**, L943 (1984).

[4]R. V. Coleman, G. Eiserman, M. P. Everson, A. Johnson, and L. M. Falicov, Phys. Rev. Lett. **55**, 863 (1985).

[5]C. A. Balseiro and L. M. Falicov, Phys. Rev. Lett. **55**, 2336 (1985).

[6]J. Friedel, Philos. Trans. R. Soc. London Ser. A **314**, 189

(1985).
[7]A. I. Buzdin, M. L. Kulić, and V. V. Tugushev, Solid State Commun. **48**, 483 (1983).
[8]T. Takahashi, D. Jérome, and K. Bechgaard, J. Phys. (Paris) Lett. **43**, L565 (1982).
[9]F. Pesty, P. Garoche, and K. Bechgaard, Phys. Rev. Lett. **55**, 2495 (1985).
[10]G. Montambaux, M. Héritier, and P. Lederer, Phys. Rev. Lett. **55**, 2078 (1985).
[11]P. Monceau, N. P. Ong, A. M. Portis, A. Meerschaut, and J. Rouxel, Phys. Rev. Lett. **37**, 602 (1976).
[12]N. P. Ong and P. Monceau, Phys. Rev. B **16**, 3443 (1977).
[13]R. M. Fleming, D. E. Moncton, and D. B. McWhan, Phys. Rev. B **18**, 5560 (1978).
[14]C. A. Balseiro, P. Schlottman, and F. Yndurain, Phys. Rev. B **21**, 5267 (1980).
[15]L. Onsager, Philos. Mag. **43**, 1006 (1952).
[16]P. G. Harper, Proc. R. Soc. London, Ser. A **68**, 874 (1955).
[17]J. Zak, in *Solid State Physics,* edited by F. Seitz, D. Turnbull, and H. Ehrenreich (Academic, New York, 1972), Vol. 27, p. 1.
[18]W. Y. Hsu and L. M. Falicov, Phys. Rev. B **13**, 1595 (1976).
[19]D. R. Hofstadter, Phys. Rev. B **14**, 2239 (1976).
[20]J. M. Luttinger and W. Kohn, Phys. Rev. **97**, 869 (1955).
[21]In the case of a very large Coulomb repulsion, where a Heisenberg-type model may be more appropiate and spin-Peierls effects arise, the transition temperature T_c may decrease as H increases, as shown in Ref. 7.
[22]C. E. T. Gonçalves da Silva and B. Koiller, Solid State Commun. **45**, 955 (1981).